A&A manuscript no.
(will be inserted by hand later)

Your thesaurus codes are:
07(02.08.1; 02.18.5; 08.03.1; 08.03.4; 08.13.2; 08.16.4)

ASTRONOMY
AND
ASTROPHYSICS
22.6.1994

Two-fluid models for stationary dust driven winds

I. Momentum and energy balance

D. Krüger, A. Gauger, and E. Sedlmayr

Institut für Astronomie und Astrophysik, PN 8-1 Hardenbergstraße 36, 10623 Berlin, Federal Republic of Germany

Received date; accepted date

Abstract. Self-consistent two-fluid models of stationary dust driven winds around cool C-stars have been calculated. The dust and the gas component are coupled by the condensation of dust from the gas phase and grain-gas collisions and are described by separate sets of equations.

It was found that in the regime of substantial mass loss where purely dust driven winds are possible the dust grains move with their equilibrium drift velocity relative to the gas. Compared to one-fluid models the dust component is dynamically diluted, leading to a decreased radiative acceleration of the wind in the outer region.

We have included detailed energy exchange rates between gas and radiation field by vibrational transitions of CO and pure rotational transitions of dipolar molecules (CO, HCN, C_2H, C_3H, CS, SiS). Our models show that frictional heating by drifting dust grains raises the gas temperature considerably above its radiative equilibrium value. This leads to significant extension of the dust condensation zone.

A sequence of models with increasing luminosities shows that the drift velocity of the dust decreases for higher luminosities. Consequently the drift related effects are more pronounced at lower luminosities.

Key words: Stars: mass loss – circumstellar matter – stars: AGB – stars: carbon – hydrodynamics – radiation mechanisms: miscellaneous

1. Introduction

The extended atmospheres of cool red giants are places of considerable dust formation accompanied by substantial mass loss. Radiation pressure on the dust grains with subsequent momentum transfer to the gas via grain-gas collisions is often discussed as a mechanism to drive these massive stellar winds (e. g. Gail & Sedlmayr 1987a, henceforth Paper III).

The question whether the photon momentum absorbed by the dust is completely transfered to the bulk of the gas, i. e. whether *complete momentum coupling* may be assumed, has been investigated by several authors and has arisen renewed interest in the last years (Gilman 1972; Berruyer & Frisch 1983; MacGregor & Stencel 1992; Netzer & Elitzur 1993). However, the results do not seem to be conclusive with regard to the momentum coupling under conditions typical of cool red giants, although the extent of this momentum coupling is vital for the validity of the stellar wind models constructed.

The question concerning the balance of the thermal energy of the gas in the presence of drifting dust grains is of equal importance, especially for the validity of the assumption of radiative equilibrium (RE). Furthermore, reasonable estimates for the temperature distribution in CDS's are required for the analysis of rotational emission and vibrational absorption lines of CO and other dipolar molecules (Keady et al. 1988; Kastner 1992). However, with regard to the modelling of dust driven winds the thermal energy balance has hitherto perceived few attention (e. g. Goldreich & Scoville 1976; Tielens 1983).

Both these questions can be answered most reliable by a two-fluid approach for the gas and the dust component: The respective components are described by separate sets of equations of balance for mass (i. e. the equations of continuity), momentum (i. e. equations of motion) and energy. These two sets of equations are coupled by transfer and exchange terms for mass, momentum and energy accounting for the condensation of dust from the gas phase and the collisional drag and frictional heating due to grain drift.

Previous investigations of two-fluid models for circumstellar dust shells (CDS) suffer from several limiting approximations and assumptions:

Send offprint requests to: D. Krüger

1. Dust formation is not treated explicitly. It is thus necessary to assign the amount of dust formed as a free input parameter.
2. The integration of the flow equation is started not at the photosphere but at an assumed, fictional radius of dust condensation instead, which is usually located in the subsonic regime of the wind (Berruyer & Frisch 1983; Tielens 1983; MacGregor & Stencel 1992).
3. Sometimes, the integration of the flow equation is even started at or beyond the assumed location of the sonic point, i. e. the transition of the wind from subsonic to supersonic is not treated and the pressure gradient in the equation of motion for the gas is neglected (Netzer & Elitzur 1993).
4. The equation of motion for the dust component is not solved explicitly. The dust is assumed to move with its equilibrium drift velocity relative to the gas instead (Tielens 1983; Netzer & Elitzur 1993).
5. The energy equation of the gas is not treated. Instead the gas temperature is assumed to be constant or decreasing according to an inverse power law (all the aforementioned except Tielens 1983).

All of these simplifications lead to an additional number of free input parameters such as mass loss rate and gas-to-dust ratio of the stellar wind in excess of the basic stellar parameters. In varying these input parameters independently the physical interrelation between them is neglected and the derived dependencies of characteristic wind quantities (e. g. terminal velocities) on those parameters may not be reliable.

It is the aim of this paper to model CDS's with as few limiting approximations as possible and in a self-consistent way, simultaneously treating the coupled system of hydrodynamics, thermodynamics, chemistry and dust formation. We consider the case of a stationary two-component outflow from a cool carbon star. Consequently, we cannot model the influence of stellar pulsations and shock waves, which are infered to be present from observations of C–rich long–period and Mira–variables and from theoretical models of their CDS's (e.g. Fleischer et al. 1992). Furthermore, we simplify the treatment of the process of dust formation by the assumption of instantaneous growth of the condensing nucleation seeds to dust grains with a uniform final radius.

The equations for the problem are formulated in Sect. 2. In Sect. 3 the boundary conditions for the problem are given and the method of solution is described. In Sect. 4 we discuss the resulting structure of a typical model, address the question of momentum coupling between grains and gas as well as the thermal energy balance of the gas and investigate the dependence of characteristic quantities on the stellar luminosity and the adopted uniform grain size. The conclusions are given in Sect. 5.

2. Basic equations

2.1. Two-fluid hydrodynamics

In this work the stellar wind is assumed to be stationary and spherically symmetric. Effects due to stellar rotation or magnetic fields are neglected.

We distinguish two components of the outflow here, namely gas and dust. While the gas can in fact be treated as a single component because of the high thermal velocities and, hence, collision rates, the dust in turn is actually a multi-component medium. There is a size distribution of grains, each moving with a different drift velocity relative to the gas. In order to treat the dust as a *single* component the assumption of a uniform grain radius $a_{\rm d}$ is introduced. For the modelling of dust formation it is therefore assumed that a newly formed condensation seed instantaneously grows to this final radius $a_{\rm d}$.

2.1.1. Gas equation of continuity

Since the mass fraction of condensable matter in red giants is of the order 10^{-3} the mass flux of the gas is unaffected by dust formation, i. e. the mass flux is conserved. Integration of the equation of continuity then yields

$$4\pi r^2 \rho_{\rm g} v_{\rm g} = \dot{M} \tag{1}$$

where the mass loss rate $\dot{M}$ is a constant and $\rho_{\rm g}$ and $v_{\rm g}$ denote the mass density and expansion velocity of the gas.

2.1.2. Dust equation of continuity

The equation of continuity for the dust component can be written as

$$\frac{1}{r^2}\frac{\mathrm{d}}{\mathrm{d}r}\left(r^2 \rho_{\rm d} v_{\rm d}\right) = m_{\rm d} J_* \tag{2}$$

where $\rho_{\rm d}$ is the mass density of the dust component and $m_{\rm d}$ the mass of a single grain which depends on the assumed final grain size $a_{\rm d}$ and the mass density ρ_s of the grain material and is given by

$$m_{\rm d} = \rho_s \frac{4\pi}{3} a_{\rm d}^3. \tag{3}$$

J_* denotes the formation rate of condensation seeds per volume element. For our calculations we adopt the expression for J_* resulting from classical nucleation theory as given by Gail & Sedlmayr (1984), being aware that the application of classical nucleation theory to carbon grain formation has been strongly critizised (Donn & Nuth 1985, cf. also Sedlmayr 1989). A more realistic approach is the formulation of the chemical pathway to carbon soot, which proceeds via formation of polycyclic aromatic hydrocarbons (Keller 1987, Frenklach & Feigelson 1989, Cherchneff et al. 1992). These investigations, though not providing compact expressions for the nucleation rate, indicate that carbon soot formation in stellar outflows actually takes place at gas temperatures ranging from 900 to 1100 K, whereas classical nucleation theory yields higher temperatures above about 1200 K. A discussion of how this may affect our results is given in Sect. 4.1.3.

2.1.3. Equation of motion for the gas

Neglecting selfgravitation of the shell the equation of motion for the gas in the case of a purely dust driven wind can be written as

$$\rho_{\rm g} v_{\rm g} \frac{{\rm d}v_{\rm g}}{{\rm d}r} + \frac{{\rm d}p}{{\rm d}r} = -\frac{GM_* \rho_{\rm g}}{r^2} + f_{\rm drag} \tag{4}$$

where p denotes the gas pressure, M_* is the stellar mass and $f_{\rm drag}$ is the collisional drag force exerted on the gas due to drifting dust grains. The drag force depends on the drift velocity $v_{\rm drift} \equiv v_{\rm d} - v_{\rm g}$ of the grains, and we adopt the approximate expression given by Draine (1986) which comprises both limit cases of subsonic and supersonic drift and is accurate within 1.5%

$$f_{\rm drag} = \rho_{\rm g} n_{\rm d} \pi a_{\rm d}^2 v_{\rm drift} \left(\frac{128 k T_{\rm g}}{9\pi\mu m_{\rm H}} + v_{\rm drift}^2 \right)^{\frac{1}{2}}. \tag{5}$$

Here $n_{\rm d}$ denotes the number density of grains and μ is the mean molecular weight corresponding to the number densities of H, H_2 and He (cf. Sect. 2.4).

By means of the gas equation of state (24) Eq. (4) can be cast in the form of a wind equation (Parker 1960)

$$(v_{\rm g}^2 - c_T^2) \frac{{\rm d}v_{\rm g}}{{\rm d}r} = v_{\rm g} \left[\frac{2c_T^2}{r} - \frac{GM_*}{r^2} + \frac{1}{\rho_{\rm g}} f_{\rm drag} - \frac{{\rm d}c_T^2}{{\rm d}r} \right]. \tag{6}$$

The wind equation has a critical or sonic point at the radius where $v_{\rm g}$ equals the isothermal sound velocity c_T of the gas. Special numerical techniques have to be invoked to deal with this internal singularity (cf. Sect. 3). If the pressure gradient in Eq. (4) is neglected and the solution of the flow equations is started at or beyond the sonic point, this problem does not arise.

Equation (6) is not yet in the canonical form of an ordinary differential equation (ODE), since the r. h. s. contains the derivative of the isothermal sound velocity c_T and thus is dependent on the temperature gradient. Neglecting the radial variation of the mean molecular weight μ the temperature gradient can be eliminated from Eq. (6) by insertion of the relevant form of the energy equation (10) (cf. Sect. 2.2.1). Some calculus yields

$$(v_{\rm g}^2 - c_S^2) \frac{{\rm d}v_{\rm g}}{{\rm d}r} = \tag{7}$$
$$v_{\rm g} \left[\frac{2c_S^2}{r} - \frac{GM_*}{r^2} + \frac{1}{\rho_{\rm g}} f_{\rm drag} - \frac{2}{f \rho_{\rm g} v_{\rm g}} (q_{\rm rad} + q_{\rm fric} + q_{\rm acc}) \right]$$

where $c_S \equiv \gamma^{-1/2} c_T$ is the *adiabatic* sound velocity of the gas. The various heating and cooling rates q_i and the mean degree of freedom f of the gas will be introduced in Sect. 2.2.1.

2.1.4. Equation of motion for the dust

For uniform grain size the equation of motion for the dust can be written as

$$\rho_{\rm d} v_{\rm d} \frac{{\rm d}v_{\rm d}}{{\rm d}r} = \frac{4\pi}{c} \kappa_H^{\rm d} H - \frac{GM_* \rho_{\rm d}}{r^2} - f_{\rm drag} + m_{\rm d}(v_{\rm inj} - v_{\rm d}) J_* \tag{8}$$

where H is the frequency integrated stellar flux (cf. Sect. 2.3) and $\kappa_H^{\rm d}$ denotes the flux mean of the dust opacity.

Within the framework of our model of instantaneous growth of the newly formed grains it is somewhat problematic to fix the injection velocity $v_{\rm inj}$ of these grains. The original nucleation seeds are small clusters comoving with the gas. During their growth they move with the velocity $v_{a(t)}$ corresponding to their momentary size $a(t)$. As the grains approach their final size $a_{\rm d}$ so does their velocity $v_{a(t)}$ with regard to $v_{a_{\rm d}}$, i. e. $v_{\rm d}$. Thus, the injection velocity of particles of size $a_{\rm d}$ is practically equal to $v_{\rm d}$ and the last term in Eq. (8) vanishes.

2.2. Thermodynamics

2.2.1. Gas energy equation

With $e_{\rm g}$ being the thermal energy per unit volume the corresponding equation of balance is

$$\frac{1}{r^2} \frac{\rm d}{{\rm d}r} \left(r^2 e_{\rm g} v_{\rm g} \right) + \frac{p}{r^2} \frac{\rm d}{{\rm d}r} \left(r^2 v_{\rm g} \right) = q_{\rm rad} + q_{\rm fric} + q_{\rm acc}. \tag{9}$$

The source terms on the r. h. s. describe the energy exchange $q_{\rm rad}$ with the radiation field, the frictional heating $q_{\rm fric}$ due to drifting dust grains and the energy exchange $q_{\rm acc}$ due to temporary accomodation of gas particles on the surface of dust grains. Other effects, e. g. exothermic chemical reactions on the surface of dust grains, are neglected.

By means of the caloric equation of state for the ideal gas and neglecting the radial variation of the mean molecular weight μ Eq. (9) can be transformed into an ODE for the kinetic gas temperature

$$\frac{{\rm d}T_{\rm g}}{{\rm d}r} = -\frac{2}{f} \frac{T_{\rm g}}{v_{\rm g}} \left(\frac{2v_{\rm g}}{r} + \frac{{\rm d}v_{\rm g}}{{\rm d}r} \right) + \frac{2}{f} \frac{\mu m_{\rm H}}{\rho_{\rm g} k v_{\rm g}} (q_{\rm rad} + q_{\rm fric} + q_{\rm acc}) \tag{10}$$

where the velocity gradient ${\rm d}v_{\rm g}/{\rm d}r$ is given by Eq. (7). In Eq. (10) f denotes the mean degree if freedom of a gas particle and is approximated by

$$f = \frac{3n_{\rm H} + 5n_{\rm H_2} + 3n_{\rm He}}{n_{\rm H} + n_{\rm H_2} + n_{\rm He}} \tag{11}$$

2.2.2. Energy exchange between gas and radiation field

In the cool and tenous shells of C-stars virtually no ionisation or electronic excitation takes place (Tsuji 1966). Thus, radiative cooling or heating is the result of vibrational and pure rotational transitions of molecules with permanent dipole moment (e. g. CO, HCN). For the present investigation we consider the following radiative energy exchange processes:

1. destruction or creation of thermal energy by collisionally induced transitions between vibrational levels of CO, which are strongly coupled to the radiative energy pool and
2. emission or absorption of photons by transitions between rotational states of various dipolar molecules (CO, HCN, C_2H, C_3H, CS, SiS), which are strongly coupled to the thermal energy pool of the gas.

We have thus neglected the pumping of rotational levels via radiative transitions to higher vibrational levels followed by radiative relaxation to higher rotational levels in the ground vibrational state. The rates $q_{\rm vib}$ and $q_{\rm rot}$ corresponding to the processes 1. and 2. are derived in the Appendix, neglecting optical depth effects in the lines, i. e. for the optically thin limit case.

A proper calculation of radiative energy exchange rates requires the solution of the radiative transfer problem for molecular lines. In principle, this involves the performance of comoving frame radiative transfer calculations, which is far beyond the scope of this paper. Within the framework of the Sobolev approximation this problem can also be dealt with by the introduction of a *local* escape probability β (Castor 1970). This is based on the fact that outside a specific resonance zone the relevant absorption lines have experienced a large enough Doppler-shift inhibiting self-absorption and allowing the emitted photons to escape. Conversely, only photons emitted inside this region contribute to the local mean intensity $J_{\rm line}$ in the spectral region of the line at the central point of the considered resonance zone. Thus, the actual net cooling rate is to a good approximation given by the product of (A2) and an escape probability β which depends on the local velocity gradient.

Calculations which make use of this escape probability formalism but neglect irradiation of the stellar photosphere or the surrounding dust shell have been performed for the outer shells of oxygen-rich red giants by Goldreich & Scoville (1976) and Tielens (1983). Their investigations indicate that due to the inclusion of the escape probability the equation of motion and the thermal energy equation of the gas can no longer be transformed in the canonical form of ODE's.

In order to circumvent the resulting numerical difficulties we have in a first step fixed the escape probability at $\beta = 1$. This amounts to assuming the spectral distribution of J to follow a Planck function $B_\lambda(T_{\rm rad})$. We are thus neglecting optical depth effects in the lines. Regarding radiative energy exchange this is not as bad an approximation for the vibrational lines. Although the optical depth $\tau_{\rm line}$ of these lines is of the order 10^3, the thermalization optical depth $\tau_{\rm th} \sim 10^5$ is even higher (Keady et al. 1988). This means the majority of the cooling photons is scattered rather than absorbed and eventually either escapes from the circumstellar envelope or is absorbed by the dust and redistributed to other frequencies than the resonance one. However, this is not true for the rotational lines for which we therefore systematically overestimate the cooling or heating efficiency. On the other hand, rotational cooling becomes important at moderate temperatures beyond the sonic point when already a considerable amount of dust has been formed (cf. Sect. 4.1.2). Since the hydrodynamical structure of the wind is rather insensitive to the temperature distribution beyond the sonic point, our results should still give a reliable picture of the CDS.

2.2.3. Frictional heating by drifting dust grains

The drifting grains do not only accelerate the bulk of the gas by momentum transfer but also heat the gas due to friction. According to Draine (1986) the corresponding rate in the case of elastic collisions and specular reflection is given by

$$q_{\rm fric}^{\rm el} = v_{\rm drift} f_{\rm drag}. \tag{12}$$

A certain fraction α of the gas particles is scattered inelastically (diffuse reflection). This means that impinging gas particles are adsorbed and thermally accomodated. Then they evaporate isotropically with a velocity distribution corresponding to the internal dust temperature $T_{\rm d}$. Since the dust is heated by the energy of the impact the frictional heating rate of the gas in the case of inelastic collisions is only half of $q_{\rm fric}^{\rm el}$ (Draine 1980). Summing up the two contributions gives

$$q_{\rm fric} = \left(1 - \frac{\alpha}{2}\right) v_{\rm drift} f_{\rm drag}. \tag{13}$$

During the accomodation of inelastically scattered gas particles internal lattice energy of the grain is transformed into thermal energy of the evaporating gas particle or vice versa, dependent on $T_{\rm g}$ being smaller or larger than $T_{\rm d}$. The corresponding energy exchange rate is given by

$$q_{\rm acc} = \alpha n_{\rm g} n_{\rm d} \pi a_{\rm d}^2 \frac{f}{2} k (T_{\rm d} - T_{\rm g}) \left(\frac{64 k T_{\rm g}}{\pi \mu m_{\rm H}} + v_{\rm drift}^2\right)^{\frac{1}{2}} \tag{14}$$

(Draine 1980). For molecular gases with a temperature of the order 10^3 K α is approximately 0.1 (Hollenbach and McKee 1979).

2.2.4. Internal energy of the dust

Since the dust component is a pressure-less medium, only the internal energy of the dust is relevant for the energy balance. This energy can be characterized by an internal lattice temperature $T_{\rm d}$ of the grains. In principle this temperature can be determined by an ODE similar to Eq. (10). It can be shown, however, that the energy exchange rate with the radiation field is several orders of magnitude larger than all other cooling or heating processes (e. g. Gauger et al. 1990). Then the internal dust temperature is simply given by the RE temperature defined in Sect. 2.3

$$T_{\rm d} = T_{\rm rad}. \tag{15}$$

2.3. Continuum radiative transfer

The stellar flux is generated in regions well below the photosphere. Since the flux of both the kinetic and the thermal energy of the flow is negligible compared to the radiative flux no significant amount of energy is added or substracted from the radiation field[1]. Then the equation of flux conservation can be integrated to give

$$H = \frac{\sigma_{\rm R} T_*^4}{4\pi} \left(\frac{R_*}{r}\right)^2 \tag{16}$$

A semi-analytical method to describe radiative transfer in extended circumstellar shells has been developed by Lucy (1971). The basic idea is to close the system of moment equations for the radiation field by splitting the specific intensity $I_\nu(r,\mu)$ of the radiation into two contributions. One part comes directly from the solid angle

$$\mu_* = \sqrt{1 - \frac{R_*^2}{r^2}} \tag{17}$$

filled by the stellar photosphere and the other part comes from the corresponding complementary solid angel. Then the first-order moment equation can be solved analytically yielding

$$J = \frac{\sigma_{\rm R} T_*^4}{2\pi} \left(1 - \mu_* + \frac{3}{2}\tau_L\right) \tag{18}$$

for $r > R_*$, where τ_L is some kind of diluted optical depth variable defined by

$$\frac{{\rm d}\tau_L}{{\rm d}r} = -(\kappa_H^{\rm g} + \kappa_H^{\rm d})\frac{R_*^2}{r^2}. \tag{19}$$

Due to the frequency integrated treatment of continuum radiative transfer the spectral distribution of the stellar flux is not known. Therefore the flux means of the gas and the dust opacity are replaced by their respective Rosseland means. The Rosseland mean $\kappa_{\rm R}^{\rm g}$ of the gas has been interpolated from tables provided by Scholz (Scholz & Tsuji 1984). If the grain radius $a_{\rm d}$ is small compared to the relevant wavelengths involved we can calculate $\kappa_{\rm R}^{\rm d}$ in the small particle limit of Mie theory

$$\kappa_{\rm R}^{\rm d} = \frac{3}{4}\frac{\rho_{\rm d}}{\rho_s} 5.9 T_{\rm rad}. \tag{20}$$

where the optical constants are adopted from Gail & Sedlmayr (1985) assuming the grains to have amorphous structure.

[1] This may not be true in variable objects where shock waves travel through the stellar shell. Here the gas is heated by dissipation of mechanical energy which is at least partially reradiated.

By means of Eq. (18) a RE temperature can be defined in the following way

$$T_{\rm rad}^4 = \frac{\pi}{\sigma_{\rm R}}\frac{\kappa_J}{\kappa_B} J \tag{21}$$

$$= \frac{T_*^4}{2}\left(1 - \sqrt{1 - \frac{R_*^2}{r^2}} + \frac{3}{2}\tau_L\right)\frac{\kappa_J}{\kappa_B} \tag{22}$$

where κ_B is the Planck mean. Assuming $\kappa_J = \kappa_B$ (grey approximation) yields

$$T_{\rm rad}^4 = \frac{T_*^4}{2}\left(1 - \sqrt{1 - \frac{R_*^2}{r^2}} + \frac{3}{2}\tau_L\right) \tag{23}$$

2.4. Gas phase chemistry

The concentrations of molecular species are of special importance for the formation of dust and the efficiency of energy exchange with the radiation field (cf. Sect. 2.2.2). For simplicity we assume chemical equilibrium in the gas phase. Then the concentrations are simply determined by the elemental abundances ϵ_i relative to hydrogen and the local pressure and kinetic temperature of the gas. In this work the concentrations of 25 molecules formed from the elements H, He, O, C, N, Fe, Si, Mg, S, and Al are calculated according to Dominik (1992).

However, there are several mechanisms which lead to deviations from chemical equilibrium (for a discussion see Goeres et al. 1988). The chemical non-equilibrium case in the winds of M-stars has been investigated by Beck et al. (1992).

The equation of state for a dilute gas is the ideal gas law

$$p = kT_{\rm g}\sum_i n_i \tag{24}$$

where n_i are the particle densities of the molecules contained in the gas. In practice, only H, H_2 and He need to be considered.

Due to the formation of carbon grains carbon is removed from the gas phase. The decrease of the corresponding abundance $\epsilon_{\rm C}$ is taken into account by the following equation

$$\frac{1}{r^2}\frac{\rm d}{{\rm d}r}\left(r^2 \epsilon_{\rm C} n_{\langle{\rm H}\rangle} v_{\rm g}\right) = -\frac{m_{\rm d}}{m_{\rm C}} J_* \tag{25}$$

where $n_{\langle{\rm H}\rangle} = n_{\rm H} + 2n_{{\rm H}_2}$ denotes the total hydrogen density and $m_{\rm C}$ is the mass of a single carbon atom.

3. Method of solution

In the previous section the two-component flow has been described by six ODE's (2), (7), (8), (10), (19) and (25) for the corresponding quantities $\rho_{\rm d}$, $v_{\rm g}$, $v_{\rm d}$, $T_{\rm g}$, τ_L and

$\epsilon_{\rm C}$. These ODE's are subject to the following boundary conditions

$$\begin{aligned} \rho_{\rm d}(R_*) &= 0 & (26)\\ T_{\rm g}(R_*) &= T_* & (27)\\ \tau_L(R_*) &= 2/3 & (28)\\ \tau_L(r\to\infty) &= 0 & (29)\\ \epsilon_{\rm C}(R_*) &= \epsilon_{\rm C,0}. & (30) \end{aligned}$$

At the onset of dust formation $v_{\rm d}$ is set to be the sum of the local gas velocity and the equilibrium drift velocity. Furthermore, an implicit internal boundary condition has to be satisfied for the wind equation (7) to remain regular at the critical point $r(v_{\rm g} = c_S)$, namely

$$\frac{2c_S^2}{r} - \frac{GM_*}{r^2} + \frac{1}{\rho_{\rm g}} f_{\rm drag} - \frac{2}{f\rho_{\rm g} v_{\rm g}}(q_{\rm rad} + q_{\rm fric} + q_{\rm acc}) = 0 \quad (31)$$

Having seven boundary conditions for a system of six differential equations we are faced with a combined eigen- and boundary value problem. This problem can be solved by the nested shooting method described in Gail & Sedlmayr (1985) and Paper III. We summarize the procedure as follows

1. The free stellar parameters M_*, L_* and T_*, the initial elemental abundances ϵ_i and the assumed grain radius $a_{\rm d}$ are fixed and a trial mass loss rate $\dot{M}$ is chosen.
2. The flow equations are integrated outwards from $r = R_*$ with a trial initial gas velocity $v_{g,0}$ which is varied until the internal boundary condition (31) is satisfied *at the sonic point*, where $v_{\rm g} = c_S$.
3. In the immediate neighbourhood (typically $\Delta r < 10^{-2} R_*$) of the sonic point the flow equations are integrated with the wind equation (7) being replaced by its analogue form (6) where, in addition, the $\mathrm{d}c_T^2/\mathrm{d}r$ term is held constant. This has the consequence that the solution slightly misses the correct sonic point. Nevertheless, this procedure forces the solution to pass from the subsonic to the supersonic region.
4. Just beyond the sonic point the integration is resumed with the wind equation (7) and with a slightly incorrect initial condition. Since, however, any solution starting somewhere close to the singular point rapidly approaches the correct solution passing through the singular point, no significant error is introduced by our method of treating the subsonic-supersonic transition (Gail & Sedlmayr 1985). At a large but finite radius, typically 30 R_*, the integration is stopped.
5. If the diluted optical depth $\tau_L(30\,R_*)$ differs significantly from zero steps 2. to 4. are repeated with a new trial mass loss rate until convergence is achieved.

In this way the complete system of non-linearly coupled equations describing a two-component dust driven wind is solved consistently. As a consequence the mass loss rate has not to be fixed *a priori* but follows as an eigenvalue of the problem.

A numerical difficulty arises from the fact that the equation of motion for the dust and the gas energy equation are *stiff* differential equations, especially in the dense regions near the photosphere. This stiffness results from the nearly vanishing differences of large source and sink terms on the r. h. s. of the respective equations. Therefore the two-component flow equations were integrated according to a three-stage fifth order implicit Runge-Kutta scheme (Hairer & Wanner 1991).

Our calculations have been performed on a Silicon Graphics IRIS Indigo R 4000 workstation. A typical model run needs about two hours of computing time.

4. Results and discussion

4.1. Structure of a typical model

For the construction of a representative or standard model of a stationary dust driven wind around a cool C-star the following parameter values have been assumed

$$\begin{aligned} L_* &= 10^4\,L_\odot & (32)\\ T_* &= 2000\,\mathrm{K} & (33)\\ M_* &= 1\,M_\odot & (34)\\ \epsilon_{\rm C,0} &= 2\,\epsilon_{\rm O} & (35)\\ a_{\rm d} &= 5\;10^{-6}\,\mathrm{cm} & (36) \end{aligned}$$

For the chemical abundance of H, He, O, N, Fe, Si, Mg, S and Al solar abundances are assumed (Allen 1973). Similar model calculations by Dominik et al. (1989) with equal stellar parameters have shown that most of the mass condensed into dust grains is concentrated around the chosen grain radius $a_{\rm d}$.

The mass loss rate resulting from a model with these parameters is

$$\dot{M} = 4.4\;10^{-6}\,M_\odot/\mathrm{yr} \quad (37)$$

which lies well within the range of 10^{-7} to $10^{-4}\,M_\odot$/yr observed for C-stars (e. g. Knapp 1987).

4.1.1. Two-component hydrodynamics

The hydrodynamical structure of the stellar envelope is presented in Fig. 1. In the upper panel the expansion velocity $v_{\rm g}$ of the gas, the isothermal sound velocity c_T and the drift velocity $v_{\rm drift}$ of the grains are shown. The lower panel depicts the forces acting on the bulk of the gas, i. e. the collisional drag force $f_{\rm drag}$ due to drifting dust grains and the pressure gradient grad p, both normated to the gravitational force.

The sharp increase of the drag force is caused by the increasing number of dust grains. Its decrease results from the reddening of the radiation field which diminishes the radiation pressure on the dust. It can be seen clearly that inside the dust shell the wind is accelerated by the pressure gradient whereas beyond the sonic point the pressure gradient contributes only little to the further acceleration of the wind.

Near the stellar photosphere the gas velocity is only several cm/s, the atmosphere nearly is in hydrostatic equilibrium. The gas velocity rises steeply with the increasing drag force and at $r = 1.5R_*$ exceeds the isothermal sound velocity which varies only weakly and is of the order of 2 km/s. Beyond the sonic point radiation pressure on dust first causes the gas velocity to further rise. Because of the drop in $f_{\rm drag}$ the gas velocity approaches a constant terminal velocity of 23.3 km/s. This value lies well within the range of 7 to 30 km/s observed for cool stellar winds (Knapp 1987).

The drift velocity of the dust is mainly dependent on the gas density and varies only slightly beyond the sonic point. It is of the order of the sound velocity. At large distance from the star there even is a small decrease of the drift velocity, since the radiation pressure on the grains is decreased due to increasing reddening of the radiation field.

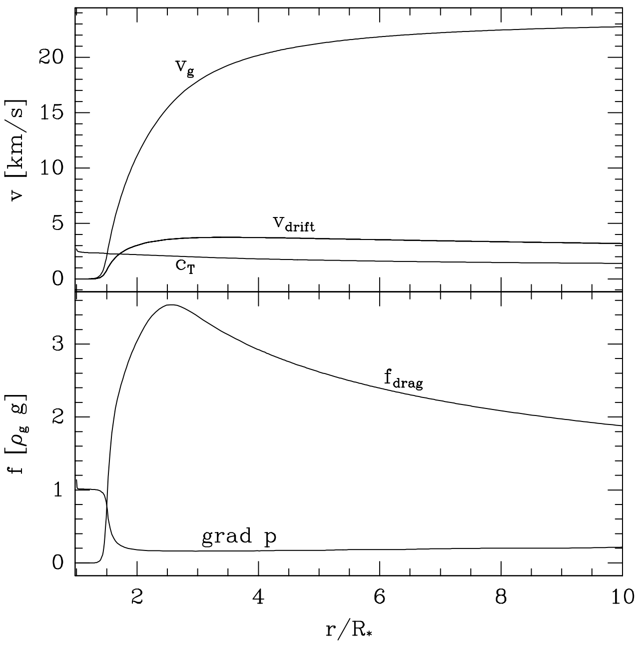

Fig. 1. Dynamical structure and acting forces for the standard model

4.1.2. Thermodynamics

Figure 2 shows the radial course of the gas temperature $T_{\rm g}$ and the RE temperature $T_{\rm rad}$ (upper panel) and the relevant cooling/heating rates normated to the gas density and multiplied with the square of the relative distance of the star $x \equiv r/R_*$ in order to eliminate changes caused solely by the geometrical dilution of the flow. Depicted are the rate of cooling $q_{\rm adb}$ due to expansion of the gas, the frictional heating rate $q_{\rm fric}$ due to drifting dust grains and the energy exchange rates with the radiation field due to vibrational transitions of carbonmonoxid $q_{\rm vib}$ and due to pure rotational transitions of the considered molecules $q_{\rm rot}$ (cf. Appendix).

At high densities or for high collision rates the gas temperature and the RE temperature are equal, the atmosphere is in RE. Just inside the sonic point the steep velocity increase and the corresponding expansion of the gas causes a pronounced cooling that cannot be completely balanced by CO vibrational heating. The gas temperature drops below the RE temperature with a maximum difference of 12 K. With the onset of dust formation the gas is additionally heated by drifting dust grains. Beyond the sonic point, $q_{\rm fric}$ is the dominant heating rate and the gas temperature is raised up to 200 K above the RE temperature.

The energy exchange with the radiation field cools the gas at a rate $q_{\rm rad} \equiv q_{\rm vib} + q_{\rm rot}$. Beyond about 2 R_* this cooling rate is dominated by rotational cooling which depends linearly on the density. The contributing molecules are mainly HCN and, to a lesser extent, CO. Only at larger distances where the chemical equilibrium concentration of HCN decreases with respect to CO, rotational cooling by CO is the dominant radiative cooling agent. However, cooling due to expansion of the gas is more efficient.

For very large distances from the star the energy balance in the CDS can be characterized by an equilibrium of adiabatic and CO rotational cooling on the one hand and frictional heating on the other hand.

The energy exchange rate $q_{\rm acc}$ due to temporary accomodation of inelastically scattered gas particles turns out to be about a factor of 10^{-2} smaller compared to the other rates and thus can be neglected throughout the CDS.

4.1.3. Dust formation

Figure 3 shows the radial course of the quantities characterizing the formation of dust. The upper panel shows the nucleation rate J_* and the corresponding increase of the number density $n_{\rm d}$ of dust grains, both normated to the total hydrogen density. The lower panel shows the ratio $\dot{M}_{\rm d}/\dot{M}_{\rm g}$ of the mass loss rates of the dust and the gas component and the corresponding decrease of the carbon abundance $\epsilon_{\rm C}$.

The mass loss rate of the dust component is given by

$$\dot{M}_{\rm d} = 4\pi r^2 n_{\rm d} m_{\rm d} v_{\rm d}. \qquad (38)$$

If $j \equiv \rho v$ denotes the mass flux density of the respective component the relative mass loss of the dust component is given by

$$\frac{\dot{M}_{\rm d}}{\dot{M}_{\rm g}} = \frac{j_{\rm d}}{j_{\rm g}} \qquad (39)$$

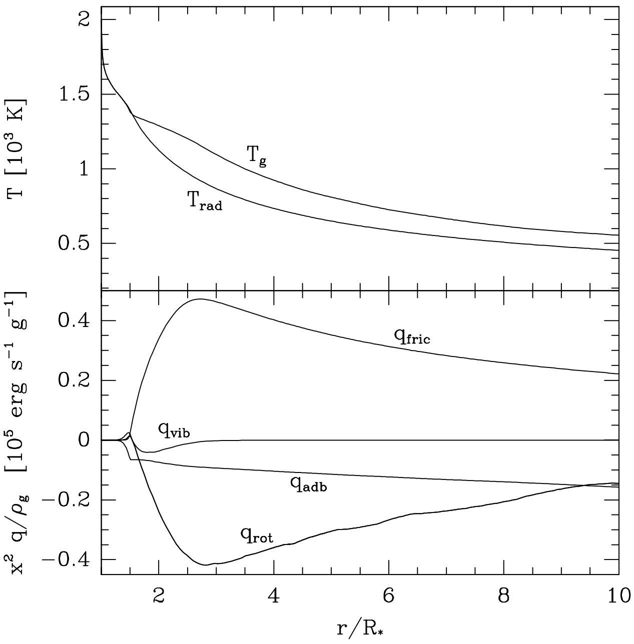

Fig. 2. Thermodynamical structure and relevant cooling/heating rates for the standard model

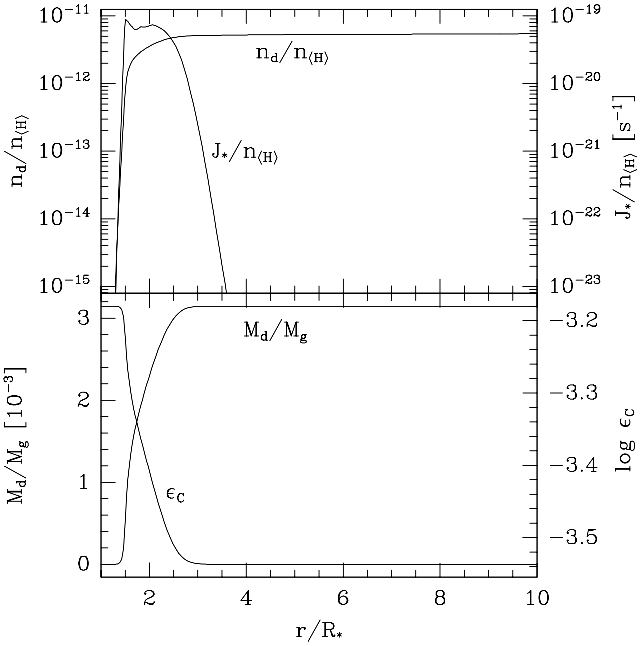

Fig. 3. Radial course of dust related quantities for the standard model

$$= \frac{\rho_{\mathrm{d}}}{\rho_{\mathrm{g}}}\left(1+\frac{v_{\mathrm{drift}}}{v_{\mathrm{g}}}\right). \tag{40}$$

We have chosen to plot this quantity, since even after completion of dust formation the ratio of dust and gas density is not a constant and thus is unsuitable to characteristize the amount of dust formed. The same is true for the degree of condensation f_{cond} usually defined as

$$f_{\mathrm{cond}} \equiv \frac{\rho_{\mathrm{d}}}{m_{\mathrm{C}}(\epsilon_{\mathrm{C},0}-\epsilon_{\mathrm{O}})n_{\langle \mathrm{H} \rangle}}. \tag{41}$$

Even in the event of complete condensation of all available carbon this quantity remains smaller then 1, since within the framework of a two-component formulation the dust component is dynamically diluted relative to the gas due to its higher velocity v_{d}.

In contrast, the mass loss ratio $\dot{M}_{\mathrm{d}}/\dot{M}_{\mathrm{g}}$ is independent of the drift velocity, since for stationary flows an increased dust velocity causes the dust density to decrease so that the mass flux density remains constant and is only determined by the amount of dust formed.

As has been found by Gail & Sedlmayr (Paper III) and Dominik (1992) dust formation takes place in a relatively small region around the sonic point. The increase of $J_*/n_{\langle \mathrm{H} \rangle}$ is due to the decreasing temperature which allows the formation of solid particles whilst the decrease of J_* can be explained by a further decreasing temperature and thus decreasing chemical equilibrium density of C_1 which is responsible for the formation of the initial nucleation seed. The intermediate minimum of J_* arises when already a relevant amount of dust is formed and the temperature is almost constant due to frictional heating, but the amount of condensable matter is reduced by the continuing dust formation. This intermediate minimum is responsible for the bend in the radial courses of ϵ_{C} and $\dot{M}_{\mathrm{d}}/\dot{M}_{\mathrm{g}}$ (cf. Fig. 3, lower panel).

Another, more realistic nucleation rate than the adopted one, which results from classical nucleation theory, has to be based on a chemical non-equilibrium formulation of the pathway to carbon soot formation. Recent investigations of this kind (e. g. Cherchneff et al. 1992) indicate, that the nucleation rate will peak at lower temperatures, i. e. larger radii. As a result, the location of the dust condensation zone and the sonic point will be shifted outwards. However, the overall picture of a dust driven wind remains essentially unchanged, since it is determined by the fact that efficient dust formation takes place and not so much by the particular chemical processes of its formation.

The mass ratio of dust to gas is $3.15\ 10^{-3}$ and within the range of values observed for C-stars (Knapp 1987). The number of grains per H-atom rises up to $5.56\ 10^{-12}$, while the carbon abundance ϵ_C drops to $2.91\ 10^{-4}$.

In Fig. 4 the Rosseland mean mass opacities of the gas and the dust are presented. Also depicted are the diluted optical depth τ_L and the optical thickness of the dust shell at $\lambda = 1\,\mu$m. The latter is given by

$$\tau_{1\mu} = \int_{R_*}^{r} \kappa_{1\mu}^{\mathrm{d}}\,\mathrm{d}r. \qquad (42)$$

The opacity of the dust can be expressed according to the results of Mie theory for small particles ($a_\mathrm{d} < \lambda/2\pi$) by

$$\kappa_\lambda^{\mathrm{d}} = n_\mathrm{d} 4\pi a_\mathrm{d}^2 \frac{2\pi a_\mathrm{d}}{\lambda} \mathrm{Im}\left\{\frac{m^2-1}{m^2+2}\right\} \qquad (43)$$

where m is the complex refractive index of the material. According to experimental results of Maron (1990) $m = 1.799 + 0.228i$ for amorphous carbon at $\lambda = 1\,\mu$m. The total optical depth of the dust shell is $\Delta\tau_{1\mu} = 2.82$, i. e. the dust shell is optically thick at this wavelength.

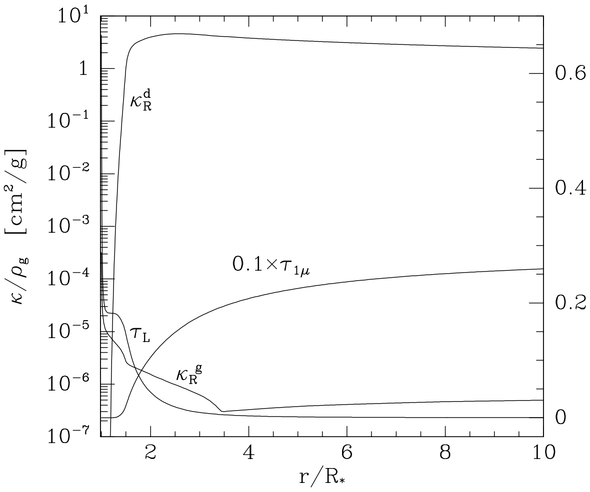

Fig. 4. Radial course of the Rosseland mean mass opacities of gas and dust, the diluted optical depth and the optical depth of the dust shell at 1 μm for the standard model

This is the reason why radiative cooling in the outer layers of our models is dominated by CO rotational line emission.

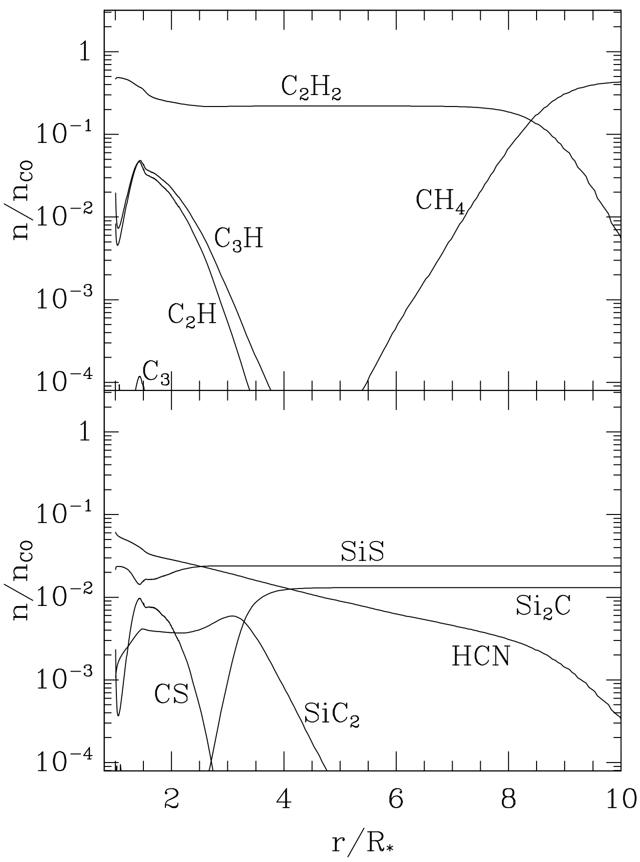

Fig. 5. Radial course of the densities of selected molecules relative to the CO density for the standard model

4.1.4. Chemistry

The chemical composition of the gas phase is shown in Fig. 5. Only the most abundant molecules (except H_2) are plotted relative to CO the concentration of which is constant and in which all the oxygen is locked. The remaining carbon is mainly in the form of acetylene. It is partly consumed by dust formation at about 2 R_*. For large distances from the star at about 10 R_*, i. e. for low temperatures, the carbon is in the form of methane. However, this is an artificial result due to our chemical equilibrium approach. Actually the densities and hence chemical reaction rates at these distances are to small to allow for efficient convertion of acetylene or other molecules by kinetic reactions.

It should be noted here that the concentration of HCN gradually decreases with increasing distance from the star.

4.1.5. Validity of complete momentum coupling

A dust driven wind is subject to the necessary condition that the radiative momentum absorbed by the dust is in turn sufficiently transfered to certain gas particles which evenly distribute the transfered momentum to the bulk of the gas. By estimating characteristic length scales Gilman (1972) showed this momentum coupling to be complete. However, a positional coupling, i. e. the assumption of equal gas and dust velocity, is generally not given.

In contrast, there are two investigations where a violation of the assumption of complete momentum coupling was found (Berruyer & Frisch 1983; MacGregor & Stencel 1992). The latter found the momentum coupling to be incomplete at mass loss rates less than $10^{-8}\,M_\odot$/yr. However, as Gail & Sedlmayr (1987b) have shown, a purely dust driven wind at such low mass loss rates is not possible even if complete momentum coupling is assumed.

Berruyer & Frisch (1983) found from their two-component models that the complete momentum coupling assumption is violated in a so-called boundary layer at their arbitrary radius of dust condensation. As a measure for this violation they used the ratio of the inertia term

$$\rho_{\rm d} v_{\rm d} \frac{{\rm d}v_{\rm d}}{{\rm d}r} \tag{44}$$

in the dust equation of motion (8) and the absolute value of the acceleration force $f_{\rm rad}^{\rm d}$, respectively. Only for *complete* momentum coupling the inertia term can be neglected relative to the acceleration and deceleration forces. In this case the drift velocity can be calculated from balancing the forces $f_{\rm rad}^{\rm d}$ and $f_{\rm drag}$.

However, the results of Berruyer & Frisch seem to be caused by the inconsistent modelling assumptions. They not only assume, as we do, instantaneous growth of the grains from the nucleation seed to their final size, but also an abrupt increase of the grain density, i. e. the nucleation rate was modelled by a delta function. The injection velocity of the newly formed grains (cf. Sect. 2.1.4) was set to be equal to $v_{\rm g}$. In other words, the growth of the dust particles has been assumed to happen instantaneously whereas their acceleration during the growth process has been followed dynamically.

This treatment does not take into account the following important points. First, during their growth the grains can adjust to increasing equilibrium drift velocities. Secondly, if the condensation zone is extended, only a small part of the dust component, namely the grains just formed, will move with the injection velocity. Only for these grains complete momentum coupling is probably violated and even this will be true only for a short time, since the dust acceleration time scale $\tau_{\rm relax}(v_{\rm d})$ is always orders of magnitude smaller than the hydrodynamic expansion time scale $\tau_{\rm exp}$. Both quantities are shown in Fig. 6 together with the relaxation time scale $\tau_{\rm relax}(T_{\rm g})$ of the gas temperature towards its equilibrium value. Thus, for the dust component as a whole momentum coupling will be still complete even if the last term in Eq. (8) is retained and $v_{\rm inj}$ is set equal to $v_{\rm g}$.

Figure 7 shows the radial course of the ratio of inertia term and accelerative force acting on the dust component

$$\xi \equiv \rho_{\rm d} v_{\rm d} \left| \frac{{\rm d}v_{\rm d}}{{\rm d}r} \right| \Big/ f_{\rm rad}^{\rm d}. \tag{45}$$

The ratio is always smaller than about $3\ 10^{-3}$, so momentum coupling is indeed complete.

To confirm our results concerning the complete momentum coupling, we have constructed a model with equal parameters where the dust velocity is always assumed to be given by the sum of the gas velocity and the equilibrium drift velocity, i. e. the equation of motion for the dust is not solved explicitly. We found no significant deviations from the original standard model.

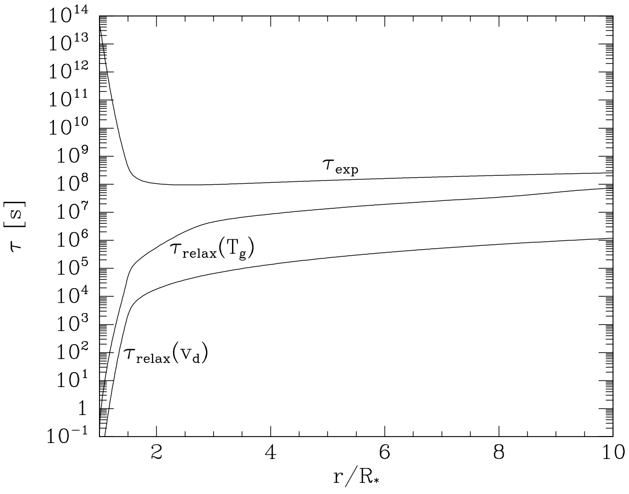

Fig. 6. Radial course of the expansion and relaxation time scales for the standard model

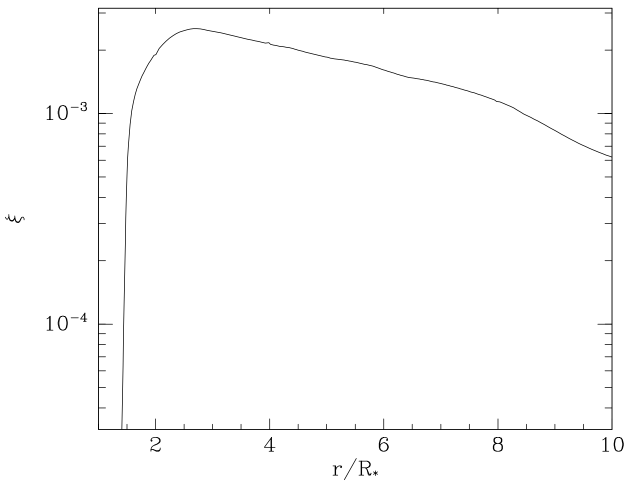

Fig. 7. Radial course of the ratio of inertia term and accelerative force of the dust component for the standard model

4.2. Comparison with the isothermal limit

Previous investigations mostly refrained from a solution of the energy equation (except Tielens 1983). Instead, RE was enforced, i. e. the gas temperature was set equal to $T_{\rm rad}$. We call this the isothermal limit case. In order to assess the importance of the energy equation we have calculated also an isothermal model with the standard parameters for comparison.

The results are presented in Fig. 8 for the dynamical (upper panel) and thermodynamical (lower panel) structure of the shell and in Fig. 9 for the dust related quantities. The dashed lines in both figures show the original standard model included for comparison. It can be seen that the dynamical structure of the wind is rather independent of the chosen approach. For the standard model gas and sound velocity are slightly smaller than for the isothermal limit case whereas the amount of dust formed is somewhat increased. The mass loss rate for the isothermal model is $\dot{M} = 4.0\ 10^{-6} M_\odot/\mathrm{yr}$ which is 10% lower than the value of the standard model.

The important differences are of course the gas temperature stratification in both models and the development of the dust condensation. The increase of the nucleation rate J_* is identical in both models. After the formation of a significant amount of dust frictional heating causes the gas temperature to decrease only slowly in the standard model resulting in an extension of the condensation zone to larger radii. Compared to the isothermal limit the inclusion of frictional heating hence leads to a broadened condensation zone shifted to larger radii.

The considerable increase of the gas temperature over the RE temperature, once dust grains are present in the circumstellar shell, clearly shows, that the energy input from the drifting grains cannot be neglected in the thermal energy balance of the gas (cf. Tielens 1983).

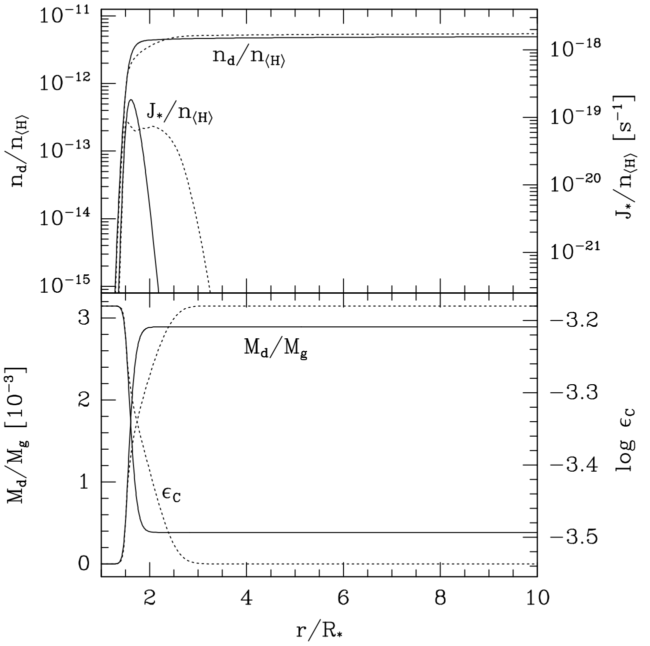

Fig. 9. Comparison of dust formation for the isothermal limit and the standard model (dashed)

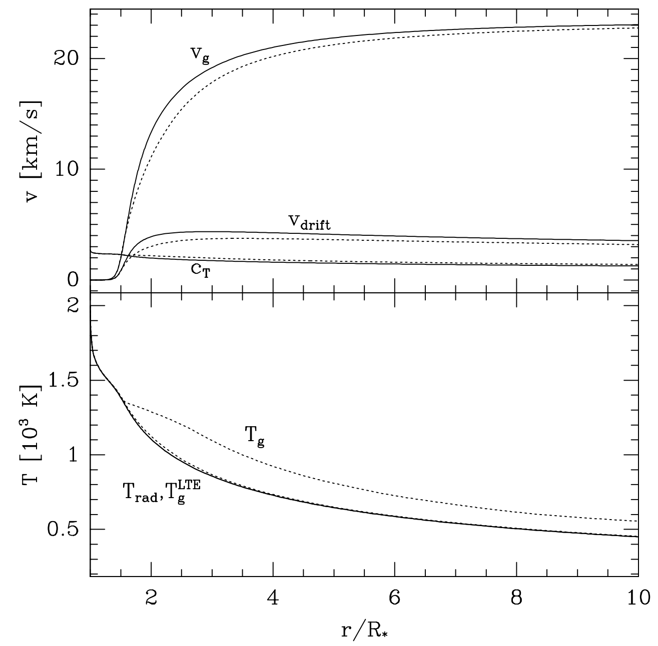

Fig. 8. Comparison of the dynamic and thermodynamic structure of the shell for the isothermal limit and the standard model (dashed)

4.3. Dependence on grain radius

Our simplified treatment of dust formation, i. e. the assumption of instantaneous growth of the newly formed dust particles, demands for an analysis of the dependence of the global wind structure and certain characteristic quantities on the free input parameter a_d. We have calculated wind models for grain sizes between 12.5 nm and 0.4 μm with the other parameters being those of the standard model. Calculations for dust driven winds which include a treatment of dust growth but neglect drift (Paper III, Dominik et al. 1989) show that in most models the mean grain size is lower than 1 μm.

We found that the general structure of the wind is unchanged by the variation of the grain size. The velocity profile is of similar shape, the position of the sonic point varies less than 1% and frictional heating causes a significant rise of the gas temperature over its RE value after the onset of dust formation.

However, the values of certain quantities characteristic for the model do change. In Figs. 10 and 11 we have plotted the dependence on the grain radius a_d for the following characteristic quantities

1. Figure 10:
   (a) the maximal ratio α_max of f_drag and $\rho_\mathrm{g} g$
   (b) the terminal velocity $v_{\mathrm{g},\infty}$ of the wind
   (c) the mass loss rate $\dot{M}$
   (d) the ratio of dust and gas mass loss rate $\dot{M}_\mathrm{d}/\dot{M}_\mathrm{g}$
2. Figure 11:
   (a) the maximal drift velocity v_drift of the dust
   (b) the maximal positive deviation of the gas temperature from its RE value due to frictional heating $\Delta^+ T$ and the maximal negative deviation $\Delta^- T$ due to adiabatic cooling inside the sonic point
   (c) the maximal ratio ξ_max of inertia term and accelerative force of the dust component
   (d) the optical depth of the dust shell $\Delta\tau_{1\mu}$ at $\lambda = 1\ \mu$m

The drift velocity increases with grain radius, since the decelerating drag force $f_{\rm drag}$ is proportional to the surface of the grain whereas the accelerating radiation pressure is proportional to its volume (cf. Eqs. (5) and (20)). The frictional heating ($\Delta^{+}T$) thus also rises because it is mainly dependent on the square of the drift velocity. Correspondingly, the temperature deviation $\Delta^{-}T$ due to expansion is weaker for larger grain size, since frictional heating already dominates at smaller radii.

The course of $\dot{M}_{\rm d}/\dot{M}_{\rm g}$ shows that the amount of condensed material increases for larger grain sizes. This is to be expected from the simplified treatment of dust formation, since for comparable condensation rates larger grains result in a larger total dust mass. Since the amount of condensable matter is limited, $\dot{M}_{\rm d}/\dot{M}_{\rm g}$ cannot exceed a limit value of about $5\;10^{-3}$ and consequently this quantity saturates for large grain radii.

The increase in $\dot{M}_{\rm d}/\dot{M}_{\rm g}$ is reflected in the increasing optical depth of the shell and for small and medium grain sizes also in the rise of $\alpha_{\rm max}$, since under the assumption of $f_{\rm drag} \approx f^{\rm d}_{\rm rad}$ this quantity is proportional to $\kappa^{\rm d}_{\rm R}$ and thus $\rho_{\rm d}$. For large grain sizes, however, the dynamical dilution of the dust component due to the increased drift velocity dominates the slow increase of the amount of dust $\dot{M}_{\rm d}/\dot{M}_{\rm g}$. Therefore, $\alpha_{\rm max}$ reaches a maximum at $a_d \approx 10^{-5}$ cm and decreases again at larger grain sizes. The terminal velocity of the wind reflects the radial course of $\alpha_{\rm max}$ since $v_{\rm g,\infty}$ is mainly determined by the momentum input beyond the sonic point (Holzer & MacGregor 1986) which is characterized by $\alpha_{\rm max}$.

The mass loss rate depends on the momentum input of the radiatively accelerated dust inside the sonic point (Holzer & MacGregor 1986). At the sonic point the internal boundary condition Eq. (31) requires $\alpha \approx 1$. For the amount of dust corresponding to this value of α it is not important whether it consists of few large or many small particles. Thus, the mass loss rate is only weakly dependent on the grain size parameter.

Since $\xi_{\rm max}$ was always of the order of a few 10^{-3}, momentum coupling is practically complete for all grain sizes under consideration.

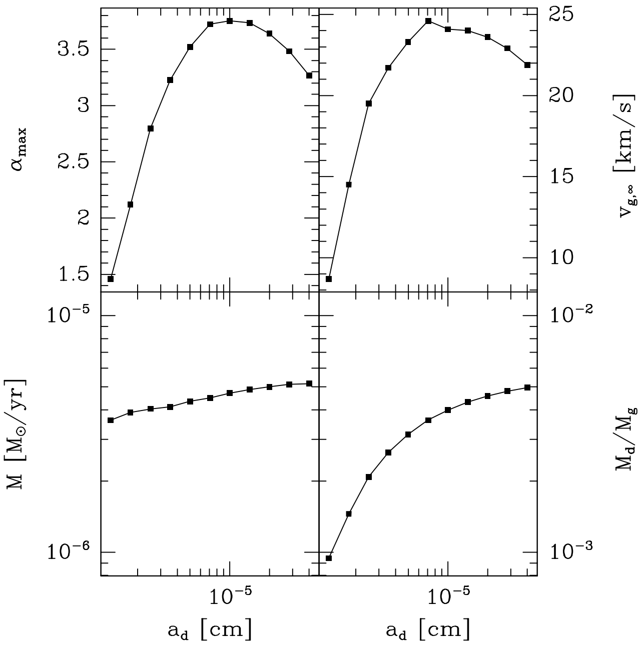

Fig. 10. Dependence of characteristic quantities (1.) on the grain radius $a_{\rm d}$

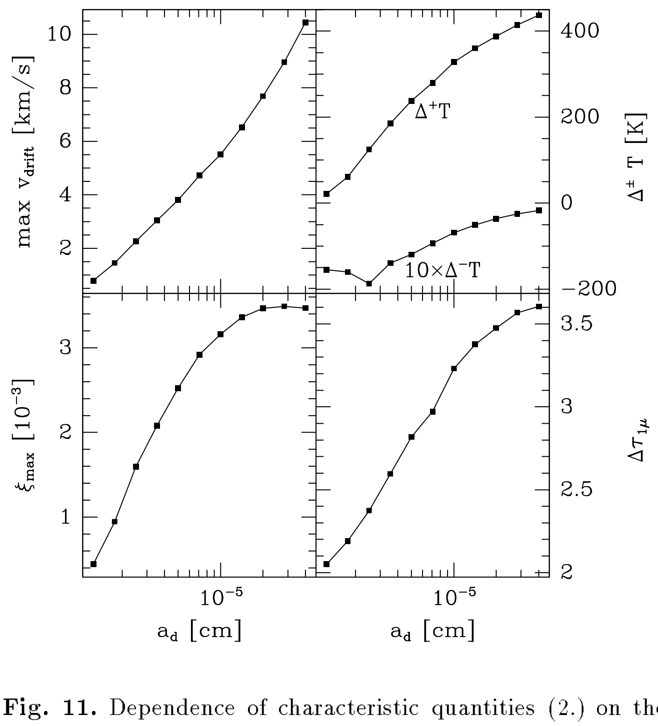

Fig. 11. Dependence of characteristic quantities (2.) on the grain radius $a_{\rm d}$

4.4. Dependence on luminosity

The domain of dust driven winds in the Hertzsprung-Russel diagram (HRD) is situated at the asymptotic giant branch (AGB). There the evolutionary path of a star leads from low (some $10^3\,L_\odot$) to high luminosities (some $10^4\,L_\odot$) with slowly decreasing effective temperature. It is not before the transition to a planetary nebula that the effective temperature strongly increases at nearly constant luminosity.

In order to investigate the dependence of the shell structure on the evolutionary state of the red giant the stellar luminosity has been varied in the range from $0.66\;10^4$ to $4.13\;10^4\,L_\odot$. All other parameters have been held constant. The model sequence shows that again the general structure of the wind changes only little. However, now the dust-to-gas ratio $\dot{M}_{\rm d}/\dot{M}_{\rm g}$ is independent of the luminosity while the position of the sonic point significantly grows with L_*.

In Figs. 12 and 13 the dependence of the following characteristic quantities on the stellar luminosity is presented

1. Figure 12
   (a) the maximal ratio $\alpha_{\rm max}$ of $f_{\rm drag}$ and $\rho_{\rm g} g$
   (b) the terminal velocity $v_{{\rm g},\infty}$ of the wind
   (c) the mass loss rate $\dot{M}$
   (d) the position of the sonic point r_c
2. Figure 13
   (a) the maximal drift velocity $v_{\rm drift}$ of the dust
   (b) the maximal positive deviation of the gas temperature from its RE value due to frictional heating $\Delta^+ T$ and the maximal negative deviation $\Delta^- T$ due to adiabatic cooling inside the sonic point
   (c) the maximal ratio $\xi_{\rm max}$ of inertia term and accelerative force of the dust component
   (d) the optical depth of the dust shell $\Delta\tau_{1\mu}$ at $\lambda = 1\,\mu$m

For constant effective temperature T_* an increase in luminosity corresponds to a larger stellar radius. Thus, the gravitational acceleration at the stellar surface decreases and for a comparable amount of dust $\dot{M}_{\rm d}/\dot{M}_{\rm g}$ the radiation pressure on the dust relative to the gravitational force, i. e. $\alpha_{\rm max}$ rises. Consequently, the transfered momentum inside and beyond the sonic point increases as do the quantities $\dot{M}$ and $v_{{\rm g},\infty}$ dependent on the momentum transfer in the respective region.

For the adopted stellar mass, effective temperature, chemical composition and grain size the dependence of the logarithm of the mass loss rate on the logarithm of the stellar luminosity can be fitted by a straight line with the slope

$$\frac{{\rm d}\ \log \dot{M}[M_\odot/{\rm yr}]}{{\rm d}\ \log L_*[L_\odot]} = 1.84. \qquad (46)$$

This is in good agreement with the slope of 1.995 given by de Jager et al. (1988) which has been determined by an empirical fit of the observed mass loss rates in the HRD.

The drift velocity is reduced for higher luminosities. This seemingly contradictory result of our self-consistent modelling can be explained in the following way. The equilibrium drift velocity depends on the ratio $L_*/\dot{M}$ (cf. Dominik 1992). Since the mass loss rate rises superlinear with the luminosity (cf. Eq. (46)) this ratio *decreases* for higher luminosities. As the drift velocity decreases so does the frictional heating ($\Delta^+ T$).

For comparable expansion velocities higher mass loss rates are equivalent to higher densities in the CDS. Thus, the density dependent vibrational heating is more effective and $\Delta^- T$ is reduced for high luminosities. Although the relative amount of formed dust $\dot{M}_{\rm d}/\dot{M}_{\rm g}$ is almost constant, the absolute dust density increases due to the increased gas density and causes the optical depth of the dust shell $\Delta\tau_{1\mu}$ to rise as well.

In our models efficient dust condensation starts at a gas temperature of about 1400 K. The increased optical depth of the dust shell for high luminosities intensifies the backwarming effect of the dust component and hence the temperature of the inner regions is increased. Dust formation thus starts at larger radii and consequently the sonic point is shifted outwards.

Complete momentum coupling is valid for all investigated luminosities, since $\xi_{\rm max}$ is always of the order of a few 10^{-3}.

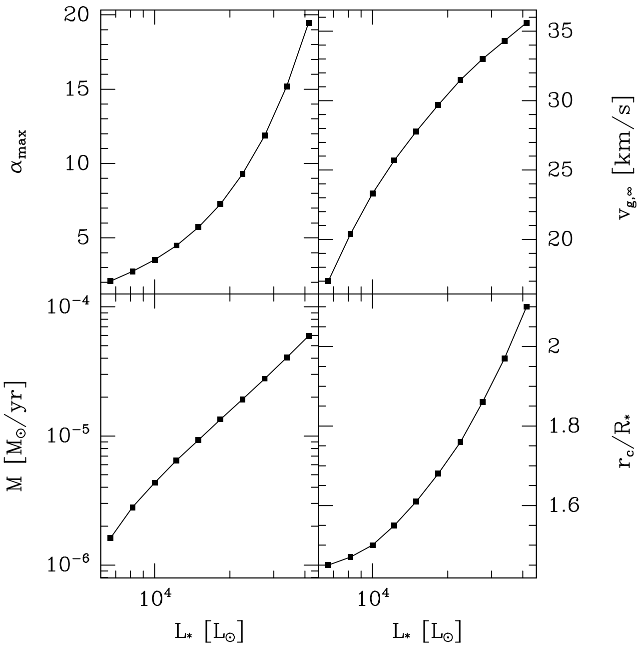

Fig. 12. Dependence of the characterisic quantities (1.) on the stellar luminosity L_*

5. Conclusions

In this work we have investigated two aspects of dust driven winds: the momentum coupling and the influence of cooling and heating processes on the radial course of the gas temperature. To do this we have described the wind by means of a two-component approach and in a self-consistent way, adopting only one parameter (the grain size $a_{\rm d}$) in excess of the basic stellar parameters. Special emphasis was laid on the modelling of the exchange and transfer terms for mass, momentum and energy between radiation field, dust and gas.

Our models confirmed the results of Tielens (1983) that the gas temperature is raised considerably over its radiative equilibrium (RE) value by frictional heating of

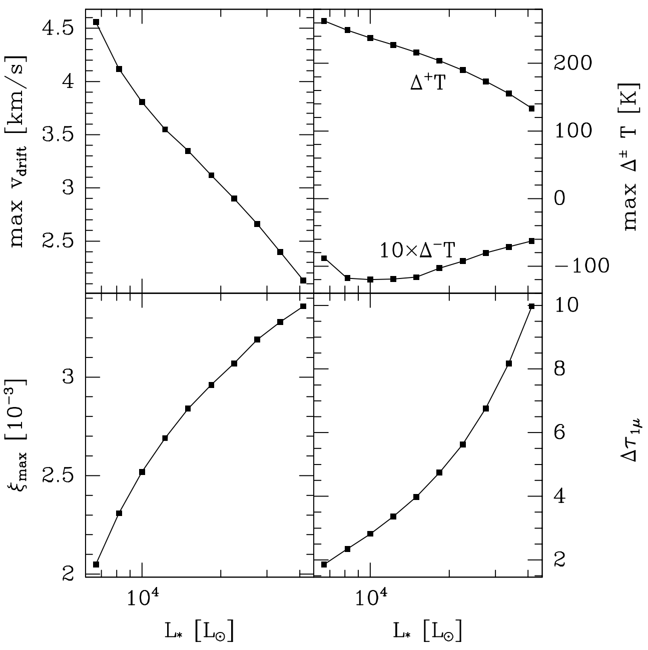

Fig. 13. Dependence of the characteristic quantities (2.) on the stellar luminosity L_*

drifting dust particles, since the gas is rather inefficient in getting rid of this energy input by line emission of dipolar molecules. Furthermore we found that the dominant cooling agents are pure rotational transitions of HCN and CO.

For comparison we calculated an isothermal model, where RE was enforced. The resulting dynamical structure and the mass loss rate of the wind were similar to those of the standard model, which included a detailed treatment of the gas energy equation. The temperature stratification, however, was clearly distinct and so was the extension of the dust condensation zone. In the standard model dust formation takes place in a broader region shifted to larger radii.

By comparison of the inertial term and the accelerative force of the dust component we have shown the momentum coupling to be complete in the regime of substantial mass loss, where purely dust driven winds are possible. This is also indicated by the ratio of the hydrodynamical expansion time scale of the wind and the acceleration time scale of the dust component. This means that the usually adopted approximation of a local equilibrium drift velocity for the grains is in fact very good. Contradictory results of Berruyer & Frisch (1983) seem to be due to an inconsistency between the treatment of the dust formation process and the acceleration of the grains during the growth to their final size.

Compared to one-fluid models the dust component is dynamically diluted, leading to a decreased radiative acceleration of the wind and an increased minimum mass loss rate necassary for a purely dust driven wind to be possible (Gail & Sedlmayr 1987b). The dynamical dilution also has to be taken into account to calculate the correct density ratio $\rho_{\rm d}/\rho_{\rm g}$ of dust and gas for given dust-to-gas ratio $\dot{M}_{\rm d}/\dot{M}_{\rm g}$.

To investigate the dependence of the wind models on the adopted parameters both the stellar luminosity L_* and the assumed radius of the grains $a_{\rm d}$ have been varied in a first step. The results mentioned above are independent of the chosen stellar luminosity and adopted final grain size, as is the general structure of the envelope, e. g. the shape of the velocity profile. However, for larger dust grains and for *lower* luminosities (resulting in a lower mass loss rate) the effects produced by the drift, such as the frictional heating of the gas, are more pronounced, because the drift velocity increases in both cases. It should be noted, that this effect is found due to our consistent modeling approach, where the mass loss rate is a result of the calculation and cannot be chosen arbitrarily. The mass loss rate scales superlinearly with the luminosity, but the drift velocity is proportional to the ratio of the luminosity and the mass loss rate. Thus, the drift velocity *decreases* with increasing luminosity.

Though comparatively advanced, our modelling of dust driven winds should be further improved:

1. The relaxation of the approximation of instantaneous growth of the newly formed dust grains is of special importance. To do this one can either modify the system of moment equations derived by Gail & Sedlmayr (1988) with regard to the position coupling of gas and dust or implement an explicit multi-component formulation, in which the size distribution function of the dust is sampled and a large number of grain sizes are treated as individual components.
2. In this paper the nucleation rate of newly formed dust grains is based on classical nucleation theory. To improve the modelling of CDS's we are in need of a compact expression for a more realistic nucleation rate resulting, for example, from a chemical pathway description of soot formation.
3. Concerning the energy exchange of dipolar molecules with the radiation field due to vibrational transitions we have treated only CO because of insufficient data for the collisional excitation cross sections of other molecules. Furthermore, the two-level model used here has to be refined for the treatment of polyatomic molecules.
   Due to our component-wise LTE approach IR-pumping of molecular rotational levels has been neglected.
   A more critical approximation is the neglection of optical depth effects, especially in the rotational lines. In order to determine the actual molecular energy level population and the efficiency of molecular line cool-

ing the radiative transfer in molecular lines has to be investigated.

4. The radiative transfer problem has been treated only in a semi-analytic, frequency integrated approximation. However, there already exist quite elaborated self-consistent dust shell models including a frequency dependent continuum radiative transfer (Winters et al. 1994) which would improve our two-component modelling approach with respect to the calculation of directly observable quantities.

Concerning the detailed treatment of dust formation and growth under the conditions of drift first investigations are under way. Preliminary results indicate that the global model characteristics vary only weakly upon the incorporation of this particular refinement of our modelling procedure. This will be the subject of a forthcoming paper.

Acknowledgements. Part of this work has been supported by the *Deutsche Forschungsgemeinschaft*, Schwerpunktprogramm: Theorie kosmischer Plasmen (grant Se 420/5-4). D. Krüger would like to thank P. Woitke and C. Dominik for helpful discussions during the revision of the manuscript.

A. Radiative energy exchange

The total rate of energy exchange of the gas with the radiation field $q_{\rm rad}$ is the sum of the contributing rates $q^i_{\rm rad}$ of the specific molecules considered.

$$q_{\rm rad} = \sum_i q^i_{\rm rad} \tag{A1}$$

For a specific molecular species i the radiative energy exchange rate is given by the difference of the total amount of absorbed and emitted energy

$$q^i_{\rm rad} = 4\pi\kappa^i_J J - 4\pi\eta^i , \tag{A2}$$

where we have assumed unit escape probability (cf. the discussion in Sect. 2.2.2). The quantities κ^i_J and η^i denote the absorption-mean opacity and the frequency integrated emissivity, respectively, of the species i. They are determined by the population densities n^i_l of the molecular energy levels (the index i will be omitted in the remainder of this section). These population densities n_l, in turn, generally result from the solution of a system of non-LTE rate equations for hundreds of molecular levels. To avoid this enormous task one often assumes LTE and calculates n_l according to the Boltzmann law. However, the LTE assumption is not valid in the extended, tenous envelopes of red giants. Because of low densities, i. e. low collision rates, radiative transitions tend to drive the matter away from LTE.

In this work we have made the *ansatz* of a component-wise LTE. This means that the population of vibrational and rotational states are decoupled (Born-Oppenheimer approximation) and are given by a Boltzmann distribution with a corresponding excitation temperature $T_{\rm vib}$ or $T_{\rm rot}$, respectively. The ratio of population densities can then be written as

$$\frac{n_{v+1,J}}{n_{v,J}} = \exp\left(-\frac{E_{v+1,J}-E_{v,J}}{kT_{\rm vib}}\right) \tag{A3}$$

$$\frac{n_{v,J+1}}{n_{v,J}} = \frac{g_{J+1}}{g_J}\exp\left(-\frac{E_{v,J+1}-E_{v,J}}{kT_{\rm rot}}\right) , \tag{A4}$$

where v and J denote the quantum number of the vibrational or rotational state, respectively, $E_{v,J}$ is the energy of the corresponding level and g_J the statistical weight of the rotational level J. This approach avoids the simplification inherent in the LTE formulation but accounts for non-LTE effects by introducing excitation temperatures $T_{\rm vib}$ and $T_{\rm rot}$. If the value of the excitation temperature is close to $T_{\rm g}$ the population of the corresponding molecular levels is rather dominated by collisions (LTE). On the other hand, an excitation temperature close to $T_{\rm rad}$ indicates that the level population is determined by the radiation field (strong non-LTE).

So far, we have reduced the problem to a determination of the excitation temperatures $T_{\rm vib}$ and $T_{\rm rot}$, respectively, for the considered molecular species. In the non-LTE case the rate equations for the population densities n_l are usually solved under the assumption of statistical equilibrium, i. e. any time or spatial derivatives vanish and the population densities are determined locally as the solution of a system of nonlinear equations. This is justified by the time scales of molecular collisional and radiative processes which are much shorter than the hydrodynamical expansion time scale. An analogous argument can be given for the equation of balance of the internal energy u of a molecular species since this energy is determined solely by the population densities of vibrational and rotational states. Then we have

$$\dot{u} = q_{\rm rad} + q_{\rm coll} \equiv 0, \tag{A5}$$

where $q_{\rm coll}$ is the energy exchange rate of the molecular species with the bulk of the gas due to collisions.

Within the framework of component-wise LTE there is no coupling between populating processes of the vibrational and rotational levels. Thus, the effects of IR-pumping of the rotational levels are neglected here. In this case Eq. (A5) is equivalent to two separate equations of internal energy balance

$$q^{\rm vib}_{\rm rad} + q^{\rm vib}_{\rm coll} = 0 \tag{A6}$$

$$q^{\rm rot}_{\rm rad} + q^{\rm rot}_{\rm coll} = 0. \tag{A7}$$

These are the implicit equations to determine $T_{\rm vib}$ and $T_{\rm rot}$, respectively, for the molecular species considered, if the expressions for $q_{\rm rad}$ and $q_{\rm coll}$ are known. We note in passing that instead of adding the radiative energy exchange contributions in Eq. (A1) one can equally well add the negative collisional exchange rates, since

$$q_{\rm rad}^{\rm vib} = -q_{\rm coll}^{\rm vib} \quad \text{and} \tag{A8}$$
$$q_{\rm rad}^{\rm rot} = -q_{\rm coll}^{\rm rot}. \tag{A9}$$

A.1. Excitation temperature of the rotational levels

To calculate the absorbed energy

$$4\pi\kappa_J^{\rm rot} J \tag{A10}$$

of a specific molecular species due to pure rotational transitions we are in need of an absorption mean $\kappa_J^{\rm rot}$ which depends both on $T_{\rm rad}$ characterizing the radiation field, and the excitation temperature $T_{\rm rot}$ which determines the internal level population.

Under the assumption of unit escape probability stated above the absorption mean can be calculated according to

$$\kappa_J^{\rm rot} = \frac{\int B_\lambda(T_{\rm rad})\kappa_\lambda^{\rm rot}(T_{\rm rot})\,{\rm d}\lambda}{B(T_{\rm rad})}. \tag{A11}$$

We have restricted ourselves to the inclusion of CO, HCN, C_2H, C_3H, CS and SiS since other molecules are either less abundant or do not have a permanent dipole moment. The absorption coefficients of these linear molecules have been calculated according to the just overlapping line (JOL) approximation (Tsuji 1966), where the specific spectral bands are smeared out to form a continuum. This assumption is not critical because only the integrated amount of energy absorbed or emitted is of interest here. The relevant molecular data have been taken from Landolt-Börnstein (Hellwege 1982) and are summarized in Table 1.

Within the framework of the component-wise LTE approach the emissivity of the specific molecular species i is simply given by the Kirchhoff-Planck law

$$\eta^{\rm rot} = \kappa_{B(T_{\rm rot})}^{\rm rot} B(T_{\rm rot}). \tag{A12}$$

The Planck mean is calculated analogous to Eq. (A11) with $T_{\rm rad}$ being replaced by $T_{\rm rot}$.

By means of the Stefan-Boltzmann law the energy exchange rate with the radiation field by rotational transitions is given according to Eqs. (A2) and (A12) after insertion of Eq. (21)

$$q_{\rm rad}^{\rm rot} = 4\sigma_R\left(\kappa_J^{\rm rot}T_{\rm rad}^4 - \kappa_{B(T_{\rm rot})}^{\rm rot}T_{\rm rot}^4\right) \tag{A13}$$

The energy exchange due to *collisional* induced pure rotational transitions is given by the sum of collisional excitation and deexcitation. Assuming that the cross-sections do not depend on the perturber, i e. collision partner, but rather on the geometric extent of the molecule i the energy exchange is given by

$$q_{\rm coll}^{\rm rot} = \sum_l\sum_{u>l} n_{\rm g}(n_l C_{lu} - n_u C_{ul})\Delta E_{lu} \tag{A14}$$
$$= \sum_l\sum_{u>l} n_{\rm g} n_l C_{ul}\left(\frac{C_{lu}}{C_{ul}} - \frac{n_u}{n_l}\right)\Delta E_{lu}, \tag{A15}$$

where $n_{\rm g}$ is the total density of collision partners or perturbers and $\Delta E_{lu} = E_u - E_l$.

The ratio of the transition rates C is given according to detailed balance arguments and the actual ratio of population densities is given by Eq. (A4). This yields

$$q_{\rm coll}^{\rm rot} = \sum_l\sum_{u>l} n_{\rm g} n_l C_{ul}\frac{g_u}{g_l}\left[\exp\left(-\frac{\Delta E_{lu}}{kT_{\rm g}}\right) - \exp\left(-\frac{\Delta E_{lu}}{kT_{\rm rot}}\right)\right], \tag{A16}$$

where the degeneracy of the rotational level J is $g_J = 2J+1$.

For the collisional transition rates C_{ul} we have adopted the following formulation by Hollenbach & McKee (1979)

$$C_{ul} \equiv \sigma_{ul}v_{\rm th} = \sigma_0\frac{n_i g_l\exp(-E_l/kT_{\rm rot})}{Z}v_{\rm th} \tag{A17}$$

where σ_0 for CO is of the order 10^{-15} cm^2, a value which has been adopted for all molecular species i. Z denotes the partition function and n_i the number density of the considered molecule i.

If the molecule is treated as a rigid rotator the rotational energy is given by

$$E_J = (J+1)JhB \approx J^2hB, \tag{A18}$$

where h is Planck's constant. Then, the partition function is given by

$$Z = \frac{kT_{\rm rot}}{hB} \tag{A19}$$

which finally yields

$$q_{\rm coll}^{\rm rot} = \frac{n_{\rm g}n_i\sigma_0 v_{\rm th}}{Z^2}\sum_l g_l\exp\left(-\frac{2E_l}{kT_{\rm rot}}\right)\sum_{u>l} g_u \left[\exp\left(-\frac{\Delta E_{lu}}{kT_{\rm g}}\right) - \exp\left(-\frac{\Delta E_{lu}}{kT_{\rm rot}}\right)\right]\Delta E_{lu} \tag{A20}$$

The summation has been truncated for $u, l > 100$.

By numerically solving Eq. (A7) the excitation temperature $T_{\rm rot}$ of the rotational levels can be determined in dependence of the gas density for various pairs of $T_{\rm g}$ and $T_{\rm rad}$. The results are shown in Figs. 14 and 15 for CO and HCN, respectively. For densities greater than $\sim 10^7$ cm^{-3} in the case of CO or greater than $\sim 10^9$ cm^{-3} in the case of HCN the rotational excitation temperatures of these molecules are solely determined by the gas temperature. The level population is dominated by collisions and thus the LTE assumption is justified. Absorbed photons are thermalized and the photons are emitted according to a Planck function at the local gas temperature. We can thus apply an LTE cooling/heating function of the form of Eq. (A13) for every molecular species i considered. The total radiative energy exchange rate due to pure rotational transitions $q_{\rm rot}$ is given by adding the contributions of all considered molecules.

$$q_{\rm rot} = \sum_i q_{\rm rad}^{{\rm rot},i} \tag{A21}$$

A proper inclusion of optical depths effects in the lines will somewhat reduce the efficiency of radiative energy exchange. Thus, the critical density at which the excitation temperature bifurcates will be shifted to lower densities. This only serves to improve our conclusion of applying an LTE cooling/heating function.

The consideration of IR-pumping of rotational levels leads to an additional radiative energy input. Consequently, radiative energy exchange is enhanced if $T_{\rm rad} > T_{\rm g}$ and decreased in the case of $T_{\rm rad} < T_{\rm g}$. With regard to Figs. 14 and 15 this means that the bifurcation of $T_{\rm rot}$ will not be symmetric to the $T_{\rm rot} = T_{\rm g}$ line anymore but skewed, rather. The curves corresponding to $T_{\rm rad} > T_{\rm g}$ will already depart from the $T_{\rm rot} = T_{\rm g}$ line at somewhat higher densities while $T_{\rm rot}$ remains equal to T_g for even lower densities if $T_{\rm rad} < T_{\rm g}$.

Table 1. Rotational constant B and dipol moment $\mu_{\rm D}$ of the considered molecules

molecule	B [MHz]	$\mu_{\rm D}$ [D]
CO	56813	0.112
HCN	44316	2.98
C_2H	43674.70	0.8
C_3H	11186.3	3.1
CS	24495.6	1.96
SiS	9102	1.73

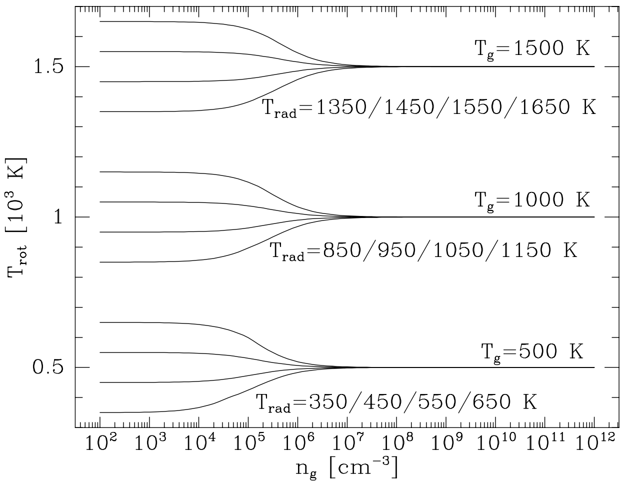

Fig. 14. Rotational excitation temperature of CO in dependence of the gas density for different pairs of gas and RE temperature

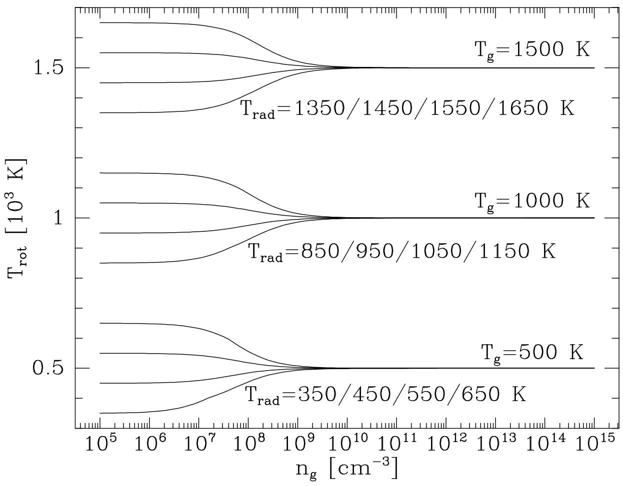

Fig. 15. Rotational excitation temperature of HCN in dependence of the gas density for different pairs of gas and RE temperature

A.2. Excitation temperature of the vibrational levels

In analogy to the derivation of Eq. (A13) in Sect. A.1 the energy exchange rate with the radiation field due to vibrational transitions is given by

$$q_{\rm rad}^{\rm vib} = 4\sigma_R \left(\kappa_J^{\rm vib} T_{\rm rad}^4 - \kappa_{B(T_{\rm vib})}^{\rm vib} T_{\rm vib}^4\right) \tag{A22}$$

To calculate the energy exchange rate $q_{\rm coll}^{\rm vib}$ due to collisional induced vibrational transitions we describe diatomic molecules by means of a two-level model (Goldreich & Scoville 1976). This approach is motivated by the following arguments

1. The collisional induced transition between vibrational levels is usually accompanied with a change of the rotational quantum number J. However, the corresponding energy difference $\Delta E_{\rm rot}$ is generally small compared to the separation of the vibrational levels $\Delta E_{\rm vib}$. Furthermore, $\Delta E_{\rm rot}$ is of varying sign depending on whether J is increasing or decreasing. Thus, one can safely assume that for the vibrational transitions the transfered energy is given by the energy separation of the ground and first excited vibrational state.
2. At the low temperatures in the CDS's of cool red giants only few molecules are in the second excited vibrational state.

Thus, for the considered molecular species we simply have

$$q_{\rm coll}^{\rm vib} = n_i h\nu_{10} n_{\rm g} C_{10} \left[\frac{C_{01}}{C_{10}} - \frac{n_1}{n_0}\right] \tag{A23}$$

$$= n_i h\nu_{10} n_{\rm g} C_{10} \left[\exp\left(-\frac{h\nu_{10}}{kT_{\rm g}}\right) - \exp\left(-\frac{h\nu_{10}}{kT_{\rm vib}}\right)\right] \tag{A24}$$

where n_i is the number density of the considered molecular species i, $h\nu_{10}$ is the energy difference between ground and first excited vibrational state and $C_{10} \equiv \langle \sigma_{10} v_{\rm th} \rangle$ is the relaxation rate per density $n_{\rm g}$ of the collision partners.

We are restricting ourselves to the treatment of CO, since the collisional relaxation rates have been obtained only for this most abundant molecule. They are usually parameterized in the following form (Ayres & Wiedemann 1989)

$$C_{10}^{\rm X,CO} = 10^{-6} k T_{\rm g} \exp(-A_{\rm X} T_{\rm g}^{-1/3} + B_{\rm X}), \qquad \text{(A25)}$$

where X denotes the specific perturber, i. e. collision partner, and $A_{\rm X}$ and $B_{\rm X}$ are the so-called Landau-Teller coefficients, which have been determined in experiments (cf. Table 2). For the chemical composition of CDS's where hydrogen is the most abundant element only the collision partners H and H_2 are relevant.

Figure 16 shows the excitation temperature $T_{\rm vib}^{\rm CO}$ of the vibrational levels of CO for a wide range of gas densities, three different gas temperatures, and four distinct differences of $T_{\rm rad}$ and $T_{\rm g}$ as it has been calculated according to Eq. (A6). In the region of moderate densities and temperatures relevant to CDS $T_{\rm vib}^{\rm CO}$ deviates only little from the RE temperature $T_{\rm rad}$. This means that the population of the vibrational levels is completely dominated by the radiation field. We are confronted with a pronounced non-LTE situation where the collisional energy transfer between CO and the bulk of the gas represents a bottleneck for radiative cooling or heating.

The energy exchange rate $q_{\rm vib} \equiv q_{\rm rad}^{\rm vib,CO}$ is to a good approximation given by

$$\begin{aligned} q_{\rm rad}^{\rm vib,CO} &= -q_{\rm coll}^{\rm vib,CO} && \text{(A26)} \\ &\approx n_{\rm CO} h\nu_{10}^{\rm CO} (n_{\rm H} C_{10}^{\rm H,CO} + n_{\rm H_2} C_{10}^{\rm H_2,CO}) \\ &\quad \left[\exp\left(-\frac{h\nu_{10}^{\rm CO}}{kT_{\rm rad}}\right) - \exp\left(-\frac{h\nu_{10}^{\rm CO}}{kT_{\rm g}}\right) \right]. && \text{(A27)} \end{aligned}$$

Table 2. Landau-Teller coefficients for CO and perturber X

Perturber X	A	B	Reference
H_2	64	19.1	Glass & Kironde 1982
H	3 ± 2	18.1 ± 0.2	Glass & Kironde 1982
He	99	20.5	Millikan & White 1964
CO	175	23.5	Millikan & White 1964

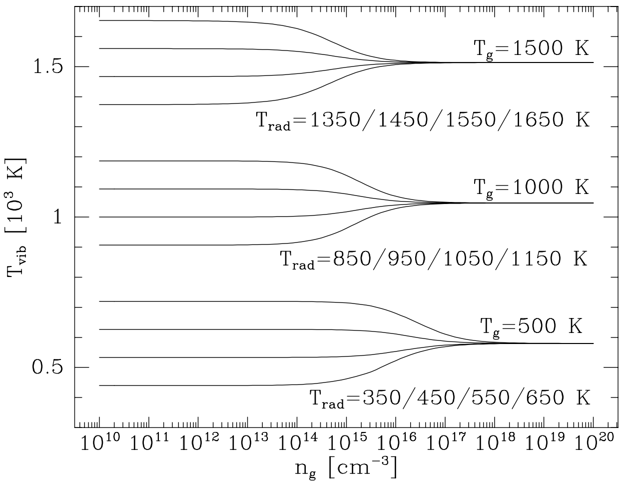

Fig. 16. Vibrational excitation temperature of CO in dependence of the gas density for different pairs of gas and RE temperature

References

Allen C.W., 1973, Astrophysical Quantities. The Athlone Press, London
Ayres T.R., Wiedemann G.R., 1989, ApJ 338, 1033
Beck H.K.B., Gail H.-P., Henkel R., Sedlmayr E., 1992, A&A 265, 626
Berruyer N., Frisch H., 1983, A&A 126, 269
Castor J.I., 1970, MNRAS 149, 111
Cherchneff I., Barker J.R., Tielens A.G.G.M., 1992, ApJ 401, 269
deJager C., Nieuwenhuijzen H., van der Hucht K.A., 1988, A&AS 72, 259
Dominik C., 1992, Formation of Dust Grains in the Winds of Cool Giants. PhD thesis, Technische Universität Berlin
Dominik C., Gail H.-P., Sedlmayr E., 1989, A&A 223, 227
Donn B., Nuth J.A., 1985, ApJ, 288, 187
Draine B.T., 1980, ApJ, 241 1021
Draine B.T., 1986, MNRAS, 220 133
Frenklach M., Feigelson E.D., 1989, ApJ, 341, 372
Fleischer A.J., Gauger A., Sedlmayr E., 1992, A&A 266, 321
Gail H.-P., Sedlmayr E., 1984, A&A 133, 320
Gail H.-P., Sedlmayr E., 1985, A&A 148, 183
Gail H.-P., Sedlmayr E., 1987a, A&A 171, 197 (Paper III)
Gail H.-P., Sedlmayr E., 1987b, A&A 177, 186
Gail H.-P., Sedlmayr E., 1988, A&A 206, 153
Gauger A., Gail H.-P., Sedlmayr E., 1990, A&A 235, 345
Gilman R.C., 1972, ApJ 178, 423
Glass G.P., Kironde S., 1982, J. Phys. Chem. 86, 908
Goeres A., Henkel R., Sedlmayr E., Gail H.-P., 1988, in: Klare G. (ed.), Rev. in Modern Astron., Springer, Berlin
Goldreich P., Scoville N.,1976, ApJ 205, 144
Hairer E., Wanner G., 1991, Solving Ordinary Differential Equations II. Springer, Berlin
Hellwege K.-H. (ed.), 1982, Landolt-Börnstein, Numerical Data and Functional Relationships in Science and Technology, vol. II/14, new series. Springer, Berlin
Hollenbach D., McKee C.F., 1979, ApJS 41,555
Holzer E.T., MacGregor K.B., 1986, in: Morris M., Zuckermann B (ed.), Mass Loss from Red Giants, Reidel, Dordrecht
Kastner J.H., 1992, ApJ 401, 337
Keller R., 1987, in: Léger A., d'Hendecourt L., Boccara N. (eds.), Polycyclic Aromatic Hydrocarbons and Astrophysics, Reidel, Dordrecht

Keady J.J., Hall D.N.B., Ridgway S.T., 1988, ApJ 326, 832
Knapp G.R., 1987, in: Kwok S., Pottasch S.R. (eds.), Late Stages of Stellar Evolution, Reidel, Dordrecht
Lucy L.B., 1971, ApJ 163, 95
MacGregor K.B., Stencel R.E., 1992, ApJ 397, 644
Maron N., 1990, Ap&SS 172, 21
Millikan R.C., White D.R., 1964, J. Chem. Phys. 39(4), 3209
Netzer N., Elitzur M., 1993, ApJ 410, 701
Parker E.N., 1960, ApJ 132, 175
Scholz M., Tsuji T., 1984, A&A 130, 11
Sedlmayr E., 1987, in: Allamandola L.J., Tielens A.G.G.M. (eds.), Interstellar Dust, IAU Symp. 135, Kluwer Academic Publishers, Dordrecht
Tielens A.G.G.M., ApJ 271, 702
Tsuji T., 1966, PASJ 18, 127
Winters J.M., Dominik C., Sedlmayr E., 1994, A&A (in press)

This article was processed by the author using Springer-Verlag LaTeX A&A style file *L-AA* version 3.